Carving out configurable ultrafast pulses from a continuous wave source via the optical Kerr effect

Fenwick, Kate L.; England, Duncan G.; Bustard, Philip J.; Fraser, James M.; Sussman, Benjamin J.

Publisher's version / Version de l'éditeur:
https://doi.org/10.1364/OE.399878
Optics Express, 28, 17, pp. 24845-24853, 2020-08-07

Research Article | Vol. 28, No. 17 / 17 August 2020 / Optics Express 24845

Optics EXPRESS

Carving out configurable ultrafast pulses from a continuous wave source via the optical Kerr effect

KATE L. FENWICK,[1,2,3] DUNCAN G. ENGLAND,[2,*] PHILIP J. BUSTARD,[2] JAMES M. FRASER,[3] AND BENJAMIN J. SUSSMAN[1,2]

[1] *Department of Physics, University of Ottawa, Ottawa, Ontario K1N 6N5, Canada*
[2] *National Research Council of Canada, 100 Sussex Drive, Ottawa, Ontario K1A 0R6, Canada*
[3] *Department of Physics, Engineering Physics & Astronomy, Queen's University, Kingston, Ontario K7L 3N6, Canada*
[*] *duncan.england@nrc-cnrc.gc.ca*

Abstract: Wavelength-tunable, time-locked pairs of ultrafast pulses are crucial in modern-day time-resolved measurements. We demonstrate a simple means of generating configurable optical pulse sequences: sub-picosecond pulses are carved out from a continuous wave laser via pump-induced optical Kerr switching in 10 cm of a commercial single-mode fiber. By introducing dispersion to the pump, the near transform-limited switched pulse duration is tuned between 305–570 fs. Two- and four-pulse signal trains are also generated by adding birefringent α-BBO plates in the pump beam. These results highlight an ultrafast light source with intrinsic timing stability and pulse-to-pulse phase coherence, where pulse generation could be adapted to wavelengths ranging from ultraviolet to infrared.

1. Introduction

Ultrafast optical technology is widespread, with a highly interdisciplinary application space including time-resolved spectroscopy [1], high-precision frequency metrology and the development of optical clocks [2], material processing and machining [3], high-speed electronic testing [4], biomedical imaging [5], and optical communications [6,7]. In time-resolved spectroscopy, *pump-probe* techniques are often used to resolve ultrafast dynamics that are too fast to be directly imaged with photodetectors. A standard pump-probe experiment utilizes one laser pulse (the *pump*) to drive the process of interest, and a second time-delayed pulse (the *probe*) to interrogate the dynamics. The pump and probe are often at different wavelengths, each depending on the system under investigation. Accordingly, generating customizable, time-locked pairs of ultrafast pulses is a crucial capability.

Often, the pump pulse is generated by a mode-locked laser and the spectrally tunable probe pulse is generated by nonlinear frequency mixing, for example in an optical parametric oscillator (OPO) or amplifier (OPA) pumped by the mode-locked laser. This is an established method for generating high-intensity probe pulses, but the bulk and expense of an OPO or OPA may be prohibitive in many cases. An alternative approach uses *all-optical switching* to carve a pulse train from a continuous-wave (CW) laser. This technique offers access to wavelengths achievable by any CW light source, including low-cost laser diodes and fiber lasers, which can be chosen appropriately for the application. Furthermore, the switching process can be driven by the pump laser to provide intrinsic timing stability. Such time-locked pulses can be generated near the pump wavelength, which would usually be challenging to achieve using an OPO or OPA. Switched pulses will necessarily be weak compared to those produced by femtosecond oscillators or nonlinear mixing, but in linear pump-probe measurements such as transient absorption or reflection, where only a differential measurement is made, high probe intensity is not required

#399878 https://doi.org/10.1364/OE.399878
Journal © 2020 Received 9 Jun 2020; revised 20 Jul 2020; accepted 30 Jul 2020; published 7 Aug 2020

Optics EXPRESS

and is often avoided [8–10]. All-optical switching of CW beams is therefore a promising option for simple, customizable ultrafast pulse generation. Picosecond-scale all-optical switching has been achieved via the optical Kerr effect [11,12], and has been demonstrated as an effective method for generating picosecond pulses in the telecommunications band around 1550 nm [13]. However, due to the length of fiber involved ($\sim 10 - 1000$ m) and the need to operate near zero dispersion, this technique is not easily implemented beyond the telecommunications band. With femtosecond lasers and short (~ 10 cm) fibers, picosecond scale all-optical switching of single photons is possible in the visible domain [14,15]. In this article, we exploit the same nonlinear process to carve light out from a CW beam, generating pulses on the hundreds-of-femtoseconds timescale, in the near-infrared.

The pulse generation technique uses a commercial mode-locked oscillator to actively induce polarization modulation in a CW laser source, by exploiting the optical Kerr effect in single-mode fiber (SMF). When the fiber is placed between two crossed-polarizers, a portion of the modulated light is transmitted, producing a sub-picosecond pulse train. This generates additional bandwidth about the narrow CW laser spectrum, which is indicative of the ultrafast switching mechanism and provides a means of characterizing the generated pulses. The method is straightforward in its implementation, where all system components are readily commercially available, and active stabilization is not necessary. Sub-nanojoule pump pulse energies are sufficient to induce the switching mechanism, falling within reach of commercial fiber oscillators, thus offering the potential for a fully integrated fiber-based optical switch. The device requires only 10 cm of conventional SMF which, combined with modest pump pulse energies, minimizes parasitic nonlinear processes such as stimulated Raman scattering, two-photon absorption, and self-phase modulation (SPM).

We achieve sequences of near transform-limited switched pulses with sub-picosecond duration, where the time-domain amplitude envelope of the pump pulse is effectively "mapped" from the carrier frequency of the pump to the signal. The switched pulse duration is tuned between 305–570 fs by introducing dispersion elements to the pump. Birefringent α-BBO plates are also added to the pump to generate trains of two and four switched pulses. Furthermore, the phase coherence of the generated pulses is expected to be time-locked for the coherence length of the CW laser. In addition to the promise of this device as an easily-implementable ultrafast light source, the demonstrations in this article underline its potential in a variety of applications including communications [16], biomedical imaging [17], microscopy [18], spectroscopy [19], and quantum optics [20].

2. Methods

Ultrafast all-optical switching relies on cross-phase modulation via the optical Kerr effect. The Kerr effect is a $\chi^{(3)}$ nonlinear process where a pump field generates an intensity-dependent refractive index modulation. The induced birefringence can be used to modulate the polarization of a signal beam. When the medium is situated between two crossed-polarizers, a portion of the modulated signal will be transmitted; this arrangement is an optical Kerr shutter [21]. For a linearly polarized pump pulse co-propagating with a CW signal beam of intensity I_0, the switched light transmitted through the shutter will have an intensity profile [22]:

$$I(t) = I_0 \sin^2(2\theta) \sin^2\left(\frac{\Delta\phi(t)}{2}\right), \tag{1}$$

where θ is the angle between the signal and pump polarization and $\Delta\phi(t)$ is the time-dependent phase difference between the polarization parallel to the pump and orthogonal to the pump. Maximal switching can only occur when $\theta = \pi/4$, so we operate under this condition. When $\Delta\phi(t) \neq 0$, the medium acts as a birefringent waveplate and allows a portion of the signal to be

Optics EXPRESS

transmitted through the second polarizer. The time-dependent phase difference is given by [23]:

$$\Delta\phi(T) = \frac{8\pi n_2}{3\lambda_{\text{signal}}} \int_0^L I_{\text{pump}}(T - d_w z)dz, \tag{2}$$

where n_2 is the nonlinear refractive index of the fiber, λ_{signal} is the wavelength of the signal light, and z is the propagation distance within the fiber of length L. In a dispersive medium, the pump and signal will experience temporal walkoff, given by $d_w = v_{gp}^{-1} - v_{gs}^{-1}$, where v_{gp} and v_{gs} are the pump and signal group velocities, respectively. As such, the intensity profile of the pump, I_{pump}, is expressed in the frame moving with the signal [15]: $T = t - z/v_{gs}$, where t is time in the laboratory frame. The switched light intensity profile is thus determined by its wavelength, the pump pulse shape, and the temporal walkoff.

An experimental schematic is shown in Fig. 1. An optical Kerr shutter is employed, where a pulsed pump beam is used to carve out pulses from a CW signal beam within 10 cm of SMF. This short fiber length was selected to achieve ultrashort, near transform-limited sub-picosecond switched pulses. A longer fiber would increase pump-signal temporal walkoff and group delay dispersion in the switched pulses. On the other hand, a shorter fiber would require higher pump pulse energies.

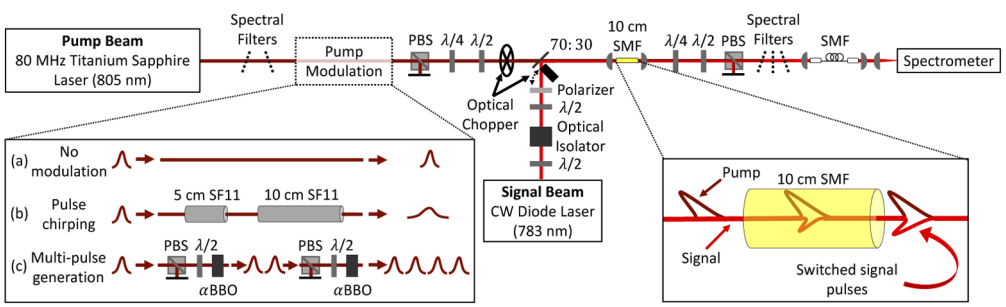

Fig. 1. Schematic diagram of the experimental setup. An 80 MHz Ti:Sapphire oscillator (pump beam) induces the optical Kerr effect in 10 cm of single-mode fiber (SMF). Shown in the bottom right inset, this mechanism carves out pulses from a continuous wave (CW) diode laser (signal beam), that are measured by a spectrometer. The pump polarization is prepared by a polarizing beamsplitter (PBS), and a quarter- ($\lambda/4$) and half-waveplate ($\lambda/2$). The signal polarization is prepared by an absorptive polarizer and $\lambda/2$ waveplate. Polarization projection of the switched light is achieved with $\lambda/4$ and $\lambda/2$ waveplates, and a PBS. Shown in the bottom left inset, pump pulses are either (a) not modulated, (b) chirped using various amounts of SF11 glass, or (c) split temporally into trains of 2 or 4 pulses using birefringent α-BBO.

The pump originates from an 80 MHz repetition rate Ti:Sapphire laser, which generates pulses of 10 nm bandwidth at a central wavelength of 805 nm. The pump is operated close to the signal spectral region to minimize temporal walkoff for sub-picosecond pulse carving. For this reason, SPM must be adequately minimized by spectral filtering of the pump prior to switching and restricting pump pulse energy. As such, the switch is operated at 30% efficiency, achieved using modest pulse energies of 0.56–1.3 nJ, depending on the pump pulse duration. After filtering, the pump pulse is measured (at the output of the SMF) to be 367 fs by frequency-resolved optical gating (FROG). As indicated by the bottom left inset in Fig. 1, the pump is prepared with either (a) no modulation, (b) temporal chirp, or (c) temporal separation into 2- and 4-pulse trains, to demonstrate the configurability of pulses generated by our switch. A polarizing beamsplitter (PBS) and a set of quarter- and half-waveplates ($\lambda/4$ and $\lambda/2$) are used to prepare the polarization state of the pump before it is combined with the signal.

Optics EXPRESS

The signal is generated by a 783 nm CW diode laser (Thorlabs CPS780S). An optical isolator (OI) is used to minimize any instability caused by back-reflection of the pump at the 10-cm SMF tip. In this configuration, the diode laser stability is sufficient for spectral measurement of the switched pulses on timescales of several minutes. A $\lambda/2$ waveplate and an absorptive polarizer prepare the initial polarization state of the signal: vertical with respect to the optical table (defined here as 0°). Both the pump and signal are chopped, at 4 Hz and 0.2 Hz respectively, for averaging and background subtraction purposes. The pump and signal are combined via a 70:30 beamsplitter and are then coupled into the 10-cm SMF (Thorlabs S630-HP, FC/PC connectors), with typical coupling efficiencies of 70% and 60%, respectively. Shown in the bottom right inset in Fig. 1, pump pulses induce birefringence while propagating through the 10-cm SMF, causing polarization-rotation in the CW signal where it temporally overlaps with the pump pulses. The output from this process is a train of pulses that have been rotated out from the initial CW signal. The switched pulses are polarization-filtered from the unswitched CW light using a PBS, which projects the signal onto a 90° (horizontal) polarization. A $\lambda/4$ and $\lambda/2$ waveplate combination are placed between the SMF and PBS to correct for small polarization changes due to the 10-cm SMF. With the pump beam blocked, these optics are tuned to minimize the CW light measured at the spectrometer. This ensures maximal transmission of the cross-polarized component of the switched light through the PBS. After polarization filtering, three angle-tuned spectral filters remove the remaining light from the pump, and the switched light is coupled into a 1-m SMF for spatial filtering of cladding modes which were not fully attenuated in the 10-cm SMF. The time-frequency relationship of optical pulses anticipates that the pulses carved from the CW signal will have larger spectral bandwidth than the narrowband input signal. Switched pulses are thus measured using a spectrometer.

Sufficient polarization extinction is required to overcome the short duty cycle of the switch. For perfect switching, a polarization extinction of ~ 10 ns/100 fs $= 10^5$ would ensure the intensities of the switched and unswitched (leakthrough) signal are on the same order of magnitude. Polarization extinction of $1.5 - 6 \times 10^4$ is achieved, causing some of the narrowband input light to leak through the second PBS. Small fluctuations in the polarization of light exiting the SMF are present due to changing air currents and vibrations, which leads to the range in measured polarization extinction values.

The integrated spectral intensity of the leakthrough is $\sim 75\times$ that of the switched signal pulse (see Fig. 2). Although this may seem insurmountable for many applications, the short duty-cycle of the switch (~ 300 fs $\times$ 80 MHz $= 2.4 \times 10^{-5}$) actually generates switched pulses with a peak intensity $\sim 3200\times$ higher than the leakthrough. Many options exist to reduce the effects of leakthrough including implementing polarizers with higher extinction ratio, increasing the repetition rate of the pump [12], employing active feedback control on the $\lambda/4$ waveplate after the SMF [24], performing nanosecond electro-optic modulation before the switch, electronic filtering using a fast detector, or even implementing a second switch. Here, background subtraction is employed to overcome the bright integrated spectral intensity of the leakthrough, where the signal and pump are periodically chopped while continuously collecting spectra. These spectra are sorted into four categories, averaged, and used to generate the switched spectrum:

$$I_{\text{switched}} = (I_1 - I_2) - (I_3 - I_4), \tag{3}$$

where I_1, I_2, I_3, and I_4 correspond to spectral data respectively sorted into categories: (1) signal on, pump on; (2) signal on, pump off; (3) signal off, pump on; and (4) signal off, pump off. Despite improvements from this method, a variable leakthrough signature still obscures the $\sim 783.0 - 783.5$ nm region and is thus excluded from all switched spectra presented in this article.

Optics EXPRESS

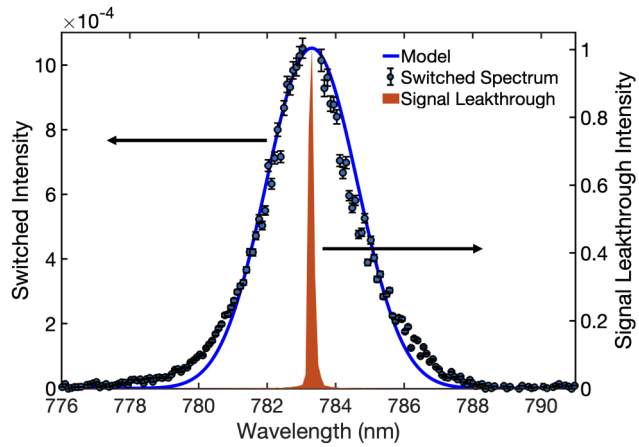

Fig. 2. Switched spectrum of generated pulses (blue data points) about the CW signal spectrum (shaded in orange) with 30% switching efficiency. Switched spectrum agrees with modelled spectrum (solid blue curve) for ~ 0.6 nJ pump pulses with 367 fs duration (measured via FROG at the 10-cm SMF output) and shows bandwidth expansion about the narrowband CW signal spectrum.

3. Results and discussion

The anticipated bandwidth expansion of the switched signal light (configuration (a) in pump modulation inset of Fig. 1) is shown in Fig. 2, where the switched spectrum is evidently broadened with respect to the signal leakthrough (input CW spectrum). Experimental data is compared with the fast-Fourier transform (FFT) of the temporal model (Eq. (1), assuming a Gaussian pump pulse of duration 367 fs) for verification and estimation of the generated pulse duration. The data and model are normalized relative to the signal leakthrough for comparison. The switched spectrum agrees with the modelled spectrum, though the model underestimates the intensity of the switched light at its tails. This is attributed to chirping of the pump pulse within the 10-cm SMF, which is not fully accounted for in the model. Given that the FFT of the model and the measured switched spectrum are in good agreement, it is inferred that the switched pulses are near transform-limited. For the experimental parameters associated with Fig. 2 ($\Delta\tau_{\text{pump}}$ = 367 fs, λ_{pump} = 805 nm, λ_{signal} = 783 nm, L_{fiber} = 10 cm, and pump pulse energy 0.6 nJ) the model estimates a generated pulse duration of 305 fs. For 30% switching efficiency, this switching window leads to generated pulse energies of ~ 0.03 fJ.

With the demonstrated ability to carve out ultrafast pulses from a CW beam and a reliable method for estimating the generated pulse duration, pump pulse modulation is introduced to demonstrate customizability of generated pulses. First, chirp is introduced in the pump pulses to control the duration of generated pulses. Pump pulses are chirped by adding 5, 10, or 15 cm of SF11 glass to the pump beam path (see (b) in pump modulation inset in Fig. 1). The addition of SF11 glass stretches the pump pulses, measured via FROG at the 10-cm SMF output, from 415 fs (no SF11 glass) to 550 fs, 675 fs, or 735 fs (with 5, 10, or 15 cm SF11, respectively). Pump pulse energies are 0.56 nJ, 0.75 nJ, 0.94 nJ, and 1.3 nJ for 0, 5, 10, and 15 cm SF11 to maintain 30% switching efficiency. As anticipated by the time-frequency relationship, narrowing in the switched spectra is observed for increasing pump pulse duration. This is shown in Fig. 3, where spectral bandwdith tunability from 1.6–2.9 nm is demonstrated. By comparing measured switched spectra to an FFT of the corresponding temporal model, measurements of generated pulse duration are again estimated (provided in Table 1). With 0–15 cm of SF11 glass, the switch is capable of generating pulses with customizable duration from 330–570 fs, where generated

Optics EXPRESS

pulses are shorter than associated pump pulses due to the quadratic sinusoidal dependency of the switching profile in Eq. (1).

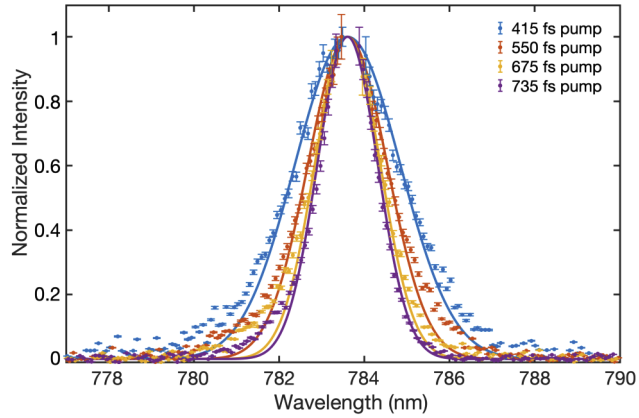

Fig. 3. Spectral bandwidth of generated pulses controlled with pump pulse duration. Switched spectra (coloured data points) agree with respective modelled spectra (matching coloured curve) for pump durations of 415 fs (blue), 550 fs (red), 675 fs (yellow), and 735 fs (purple).

Table 1. Modulation of generated pulse duration by chirping pump pulses (measured by FROG at SMF output) with SF11 glass.

SF11 Glass Added	Pump Pulse Duration (measured via FROG)	Generated Pulse Duration (estimated from model)
0 cm	415 fs	330 fs
5 cm	550 fs	435 fs
10 cm	675 fs	525 fs
15 cm	735 fs	570 fs

In addition to generating ultrafast pulses with tunable spectral bandwidth, sequences of two and four switched pulses are achieved by adding birefringent media (α-BBO crystals) to the pump beam path (see (c) in pump modulation inset in Fig. 1). Two-pulse trains are prepared using a single α-BBO crystal (with a thickness of either 5 or 10 mm), and a four-pulse train is prepared using two α-BBO crystals (of thickness 5 and 10 mm). The fast axis of the α-BBO crystals are oriented at 45° with respect to the pump polarization and components of a single pump pulse that are polarized along the fast and slow axes of a single α-BBO crystal are temporally separated into two pulses that are cross-polarized. The temporal separation is set by the thickness of the α-BBO crystal. Following each α-BBO crystal, the orthogonally polarized pulse pair is projected onto a single polarization by a PBS.

Pump pulse trains separated by some known delay, $\Delta\tau_{\text{delay}}$, carve out trains of switched pulses separated with the same delay. A train of switched pulses leads to spectral interference with fringe spacing: $\Delta\omega = 2\pi/\Delta\tau_{\text{delay}}$ [25,26]. Spectral interference in the switched spectra for three different pump pulse train sequences is measured (left column in Fig. 4) and converted to the frequency-domain using a linear interpolation, after which the IFFT can then be taken (right column in Fig. 4). The IFFT results show: (a) one peak at 2.10 ps, (b) one peak at 4.38 ps, and (c) three peaks at 2.13 ps, 4.36 ps, and 6.50 ps. These results are consistent with the generated delays predicted by the polarization-dependent group velocity of α-BBO: (a) two pulses separated by 2.15 ps, (b) two pulses separated by 4.30 ps, and (c) four pulses separated by 2.15 ps. The peak at

Optics EXPRESS

0 ps in each IFFT corresponds to the sum of the spectral profiles for all pulses present, and thus has a higher intensity than subsequent peaks corresponding to the interference [26]. These results demonstrate control over pulse sequence which, with tunable wavelength, duration, and temporal separation, could be useful, for example, in low-intensity Ramsey-comb spectroscopy [27,28].

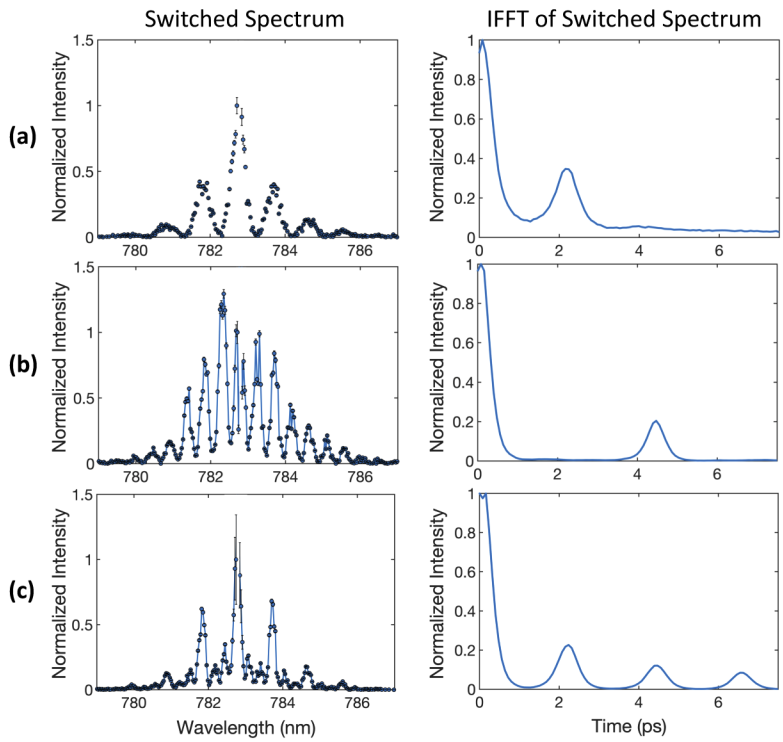

Fig. 4. Switched spectra (left) and respective IFFTs (right) for input pump trains of: (a) two pulses, separated by 2.15 ps; (b) two pulses, separated by 4.30 ps; and (c) four pulses, separated by 2.15 ps.

4. Conclusion

In summary, we demonstrated ultrafast pulse generation from a CW diode laser via the optical Kerr effect in only 10 cm of commercially available SMF. The device achieves temporally configurable pulses, and the technique provides a reliable means of switch speed characterization which can be extended to any all-optical switch [29–32]. Sub-nanojoule pump energies are sufficient and no active stabilization is required, making the implementation simple. Though switched pulse energies are low (sub-femtojoule), they are sufficient for transient pump-probe spectroscopy, and pulse characterization in the time-domain could be achieved using *temporal analysis, by dispersing a pair of light electric fields* (TADPOLE) [33]. It is expected that a range of CW sources could be implemented to achieve pulse generation over a wide range of wavelengths (i.e., 0.375–1.5 µm), noting that the signal, pump, and Kerr medium should be chosen appropriately for desired wavelength and duration of the generated pulses. The generated pulse duration is limited by the pump pulse duration and pump-signal walkoff in the Kerr medium; therefore, employing shorter pump pulses or exploiting dispersion engineering in photonic crystal fiber (PCF) could be used to generate shorter pulses. Another prospect for this device includes full fiber integration with, for example, a CW fiber laser input signal and a gigahertz fiber oscillator pump, which provides another means of reducing signal leakthrough. With some

Optics EXPRESS

modifications, this switching technique is anticipated to be beneficial in ultrafast time-gating applications including, for example, improving timing selectivity in both microscopy [34] and spectroscopy [35]. Beyond the classical realm, this is expected to be a useful tool in quantum optics, such as in the conversion of photonic qubits [14] and quantum metrology [36,37].

Funding

Natural Sciences and Engineering Research Council of Canada; University of Ottawa-NRC Joint Centre for Extreme Photonics.

Acknowledgments

The authors wish to thank Frédéric Bouchard, Khabat Heshami, Yingwen Zhang, Kent Bonsma-Fisher, Rune Lausten, Denis Guay, and Doug Moffatt for useful discussion and technical assistance.

Disclosures

The authors declare no conflicts of interest.

References

1. V. Blanchet, M. Z. Zgierski, T. Seideman, and A. Stolow, "Discerning vibronic molecular dynamics using time-resolved photoelectron spectroscopy," Nature **401**(6748), 52–54 (1999).
2. M. Takamoto, F.-L. Hong, R. Higashi, and H. Katori, "An optical lattice clock," Nature **435**(7040), 321–324 (2005).
3. K. M. Davis, K. Miura, N. Sugimoto, and K. Hirao, "Writing waveguides in glass with a femtosecond laser," Opt. Lett. **21**(21), 1729–1731 (1996).
4. A. Y. Elezzabi and M. R. Freeman, "Ultrafast magneto-optic sampling of picosecond current pulses," Appl. Phys. Lett. **68**(25), 3546–3548 (1996).
5. A. Adhikari, J. K. Eliason, J. Sun, R. Bose, D. J. Flannigan, and O. F. Mohammed, "Four-dimensional ultrafast electron microscopy: Insights into an emerging technique," ACS Appl. Mater. Interfaces **9**(1), 3–16 (2017).
6. H. C. H. Mulvad, M. Galili, L. K. Oxenløwe, H. Hu, A. T. Clausen, J. B. Jensen, C. Peucheret, and P. Jeppesen, "Demonstration of 5.1 Tbit/s data capacity on a single-wavelength channel," Opt. Express **18**(2), 1438–1443 (2010).
7. T. Morioka, K. Uchiyama, S. Kawanishi, S. Suzuki, and M. Saruwatari, "Multiwavelength picosecond pulse source with low jitter and high optical frequency stability based on 200 nm supercontinuum filtering," Electron. Lett. **31**(13), 1064–1066 (1995).
8. M. Wesseli, C. Ruppert, S. Trumm, H. J. Krenner, J. J. Finley, and M. Betz, "Nonlinear optical response of a single self-assembled ingaas quantum dot: A femtojoule pump-probe experiment," Appl. Phys. Lett. **88**(20), 203110 (2006).
9. M. Namboodiri, T. Khan, K. Karki, M. M. Kazemi, S. Bom, G. Flachenecker, V. Namboodiri, and A. Materny, "Nonlinear spectroscopy in the near-field: time resolved spectroscopy and subwavelength resolution non-invasive imaging," Nanophotonics **3**(1-2), 61–73 (2014).
10. K. Karki, M. Namboodiri, T. Zeb Khan, and A. Materny, "Pump-probe scanning near field optical microscopy: Sub-wavelength resolution chemical imaging and ultrafast local dynamics," Appl. Phys. Lett. **100**(15), 153103 (2012).
11. N. A. Whitaker, H. Avramopoulos, P. M. W. French, M. C. Gabriel, R. E. LaMarche, D. J. D. Giovanni, and H. M. Presby, "All-optical arbitrary demultiplexing at 2.5 Gbits/s with tolerance to timing jitter," Opt. Lett. **16**(23), 1838–1840 (1991).
12. E. Yamada, K. Suzuki, and M. Nakazawa, "Subpicosecond optical demultiplexing at 10 GHz with zero-dispersion, dispersion-flattened, nonlinear fibre loop mirror controlled by 500 fs gain-switched laser diode," Electron. Lett. **30**(23), 1966–1968 (1994).
13. L. Moller, Y. Su, X. Liu, J. Leuthold, and C. Xie, "Ultrahigh-speed optical phase correlated data signals," IEEE Photonics Technol. Lett. **15**(11), 1597–1599 (2003).
14. C. Kupchak, P. J. Bustard, K. Heshami, J. Erskine, M. Spanner, D. G. England, and B. J. Sussman, "Time-bin-to-polarization conversion of ultrafast photonic qubits," Phys. Rev. A **96**(5), 053812 (2017).
15. C. Kupchak, J. Erskine, D. England, and B. Sussman, "Terahertz-bandwidth switching of heralded single photons," Opt. Lett. **44**(6), 1427–1430 (2019).
16. S. Matsuo, A. Shinya, T. Kakitsuka, K. Nozaki, T. Segawa, T. Sato, Y. Kawaguchi, and M. Notomi, "High-speed ultracompact buried heterostructure photonic-crystal laser with 13 fJ of energy consumed per bit transmitted," Nat. Photonics **4**(9), 648–654 (2010).
17. S. Andersson-Engels, R. Berg, S. Svanberg, and O. Jarlman, "Time-resolved transillumination for medical diagnostics," Opt. Lett. **15**(21), 1179–1181 (1990).

Optics EXPRESS

18. G. Vicidomini, G. Moneron, K. Y. Han, V. Westphal, H. Ta, M. Reuss, J. Engelhardt, C. Eggeling, and S. W. Hell, "Sharper low-power STED nanoscopy by time gating," Nat. Methods **8**(7), 571–573 (2011).
19. P. Matousek, M. Towrie, A. Stanley, and A. W. Parker, "Efficient rejection of fluorescence from Raman spectra using picosecond Kerr gating," Appl. Spectrosc. **53**(12), 1485–1489 (1999).
20. R. Prevedel, P. Walther, F. Tiefenbacher, P. Böhi, R. Kaltenbaek, T. Jennewein, and A. Zeilinger, "High-speed linear optics quantum computing using active feed-forward," Nature **445**(7123), 65–69 (2007).
21. J. Etchepare, G. Grillon, R. Muller, and A. Orszag, "Kinetics of optical Kerr effect induced by picosecond laser pulses," Opt. Commun. **34**(2), 269–272 (1980).
22. H. Kanbara, H. Kobayashi, T. Kaino, T. Kurihara, N. Ooba, and K. Kubodera, "Highly efficient ultrafast optical Kerr shutters with the use of organic nonlinear materials," J. Opt. Soc. Am. B **11**(11), 2216–2223 (1994).
23. G. Agrawal, *Applications of nonlinear fiber optics* (Academic Press, 2001).
24. A. V. Kuhlmann, J. Houel, D. Brunner, A. Ludwig, D. Reuter, A. D. Wieck, and R. J. Warburton, "A dark-field microscope for background-free detection of resonance fluorescence from single semiconductor quantum dots operating in a set-and-forget mode," Rev. Sci. Instrum. **84**(7), 073905 (2013).
25. C. Iaconis and I. A. Walmsley, "Self-referencing spectral interferometry for measuring ultrashort optical pulses," IEEE J. Quantum Electron. **35**(4), 501–509 (1999).
26. L. Lepetit, G. Chériaux, and M. Joffre, "Linear techniques of phase measurement by femtosecond spectral interferometry for applications in spectroscopy," J. Opt. Soc. Am. B **12**(12), 2467–2474 (1995).
27. J. Morgenweg, I. Barmes, and K. S. E. Eikema, "Ramsey-comb spectroscopy with intense ultrashort laser pulses," Nat. Phys. **10**(1), 30–33 (2014).
28. L. S. Dreissen, C. Roth, E. L. Gründeman, J. J. Krauth, M. Favier, and K. S. E. Eikema, "High-precision Ramsey-comb spectroscopy based on high-harmonic generation," Phys. Rev. Lett. **123**(14), 143001 (2019).
29. H. Lu, X. Liu, L. Wang, Y. Gong, and D. Mao, "Ultrafast all-optical switching in nanoplasmonic waveguide with Kerr nonlinear resonator," Opt. Express **19**(4), 2910–2915 (2011).
30. K. Nozaki, T. Tanabe, A. Shinya, S. Matsuo, T. Sato, H. Taniyama, and M. Notomi, "Sub-femtojoule all-optical switching using a photonic-crystal nanocavity," Nat. Photonics **4**(7), 477–483 (2010).
31. Z.-G. Zang and W.-x. Yang, "Theoretical and experimental investigation of all-optical switching based on cascaded LPFGs separated by an erbium-doped fiber," J. Appl. Phys. **109**(10), 103106 (2011).
32. W. Yoshiki and T. Tanabe, "All-optical switching using Kerr effect in a silica toroid microcavity," Opt. Express **22**(20), 24332–24341 (2014).
33. D. N. Fittinghoff, J. L. Bowie, J. N. Sweetser, R. T. Jennings, M. A. Krumbügel, K. W. DeLong, R. Trebino, and I. A. Walmsley, "Measurement of the intensity and phase of ultraweak, ultrashort laser pulses," Opt. Lett. **21**(12), 884–886 (1996).
34. J. C. Blake, J. Nieto-Pescador, Z. Li, and L. Gundlach, "Ultraviolet femtosecond Kerr-gated wide-field fluorescence microscopy," Opt. Lett. **41**(11), 2462–2465 (2016).
35. S. Draxler and M. E. Lippitsch, "Time-resolved fluorescence spectroscopy for chemical sensors," Appl. Opt. **35**(21), 4117–4123 (1996).
36. J. M. Donohue, M. Agnew, J. Lavoie, and K. J. Resch, "Coherent ultrafast measurement of time-bin encoded photons," Phys. Rev. Lett. **111**(15), 153602 (2013).
37. J.-P. W. MacLean, J. M. Donohue, and K. J. Resch, "Direct characterization of ultrafast energy-time entangled photon pairs," Phys. Rev. Lett. **120**(5), 053601 (2018).